Inorganic Chemistry

ARTICLE

pubs.acs.org/IC

Palladium Complexes Affect the Aggregation of Human Prion Protein PrP106-126

Yanli Wang,[†,§] Li Feng,[‡,§] Bingbing Zhang,[†] Xuesong Wang,[†] Cheng Huang,[‡] Yiming Li,[*,‡] and Weihong Du[*,†]

[†]Department of Chemistry, Renmin University of China, Beijing 100872, China

[‡]School of Pharmacy, Shanghai University of Traditional Chinese Medicine, Shanghai 201203, China

Supporting Information

ABSTRACT: Many neurodegenerative disorders are induced by protein conformational change. Prion diseases are characterized by protein conformational conversion from a normal cellular form (PrP^C) to an abnormal scrapie isoform (PrP^{Sc}). PrP106-126 is an accepted model for studying the characteristics of PrP^{Sc} because they share many biological and physiochemical properties. To understand how metal complexes affect the property of the prion peptide, the present work investigated interactions between Pd complexes and PrP106-126 based on our previous research using Pt and Au complexes to target the peptide. The selected compounds ($Pd(phen)Cl_2$, $Pd(bipy)Cl_2$, and $Pd(en)Cl_2$) showed strong binding affinity to PrP106-126 and affected the conformation and aggregation of this active peptide in a different binding mode. Our results indicate that it may be the metal ligand-induced spatial effect rather the binding affinity that contributes to better inhibition on peptide aggregation. This finding would prove valuable in helping design and develop novel metallodrugs against prion diseases.

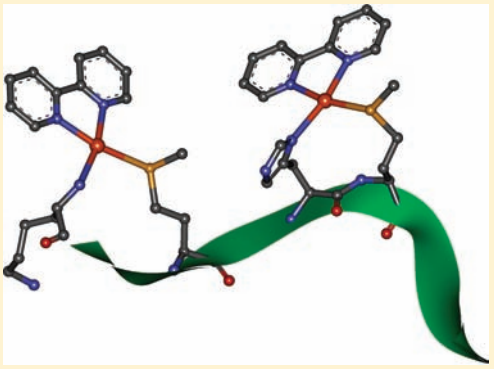

INTRODUCTION

Prion diseases are a group of fatal neurodegenerative disorders that infect both animals and humans.[1,2] They are characterized by conformational change from the normal cellular form of prion protein (PrP^C) to the abnormal scrapie isoform (PrP^{Sc}).[3] PrP^C is a membrane protein predominantly concentrated in the central nervous system, and PrP^{Sc} is defined as an infectious particle.[4,5] The two isomers are identical in the primary structure but different in their secondary structure elements. The PrP^C−PrP^{Sc} conversion results in a reduction in the α-helix content from ∼40% in PrP^C to ∼30% in PrP^{Sc} and an increase in the β-sheet content from ∼3% in PrP^C to ∼43% in PrP^{Sc}.[6] No chemical modification is induced by the conversion, but significant changes in physicochemical properties occur between PrP^C and PrP^{Sc}. Compared with PrP^C, PrP^{Sc} is resistant to protease and shows a strong tendency toward aggregating into insoluble fibrils that disrupt the neuronal function. The biological function of PrP^C is not well understood, but current experimental evidence supports PrP^C being involved in enzymatic activity and cellular signal transduction processes.[7,8]

As the full-length PrP^{Sc} is difficult to isolate and characterize, the synthetic peptide PrP106-126 (106-KTNMKHMAGAAAAGAVVGGLG-126), an N-terminal fragment of the human prion protein, has been widely used as a suitable model peptide to study the biological and physiochemical properties of PrP^{Sc}. PrP106-126 is highly conserved among various species and is suggested as the most important region in regard to initiating the conformational change, leading to the conversion of PrP^C to PrP^{Sc}.[9−11] PrP106-126 shares many physicochemical and biological properties with PrP^{Sc}, including cellular toxicity, fibrillogenesis, and membrane-binding affinity.[12,13] Furthermore, the toxicity of PrP^{Sc} and PrP106-126 requires the expression of PrP^C to cause cell death, and they can bind to PrP^C at residues 112−119.[14]

The toxicity of PrP106-126 is thought to be correlated with its primary structure. PrP106-126 is composed of two distinct regions: a hydrophilic region (K106-M112) and a hydrophobic region (A113-G126). It shows a high tendency to aggregate into the β-sheet structure, forming amyloid fibrils *in vitro* and becoming partially resistant to proteolysis.[15,16] Recent studies reported that the oligomerization of PrP106-126 resulted from the association of ordered β-hairpin monomers rather than disordered monomers.[17,18] Another study revealed that early ordered oligomers were stacked by the interface of hydrophobic C-terminal residues (A113-G126), which might increase the rate of fibril growth and form the fibril structure.[19]

The relationship between the amyloid structure and its peptide toxicity implies that PrP106-126 toxicity might be inhibited in case of failure to form the amyloid structure. A number of experimental data demonstrated that divalent metal cations binding to PrP106-126 modulated its aggregation and neurotoxic properties,[20−23] and the imidazole side chain of His111 was

Received: November 22, 2010
Published: April 19, 2011

Scheme 1. Structures of Pd Complexes: Pd(phen)Cl_2 (a), Pd(bipy)Cl_2 (b), and Pd(en)Cl_2 (c)

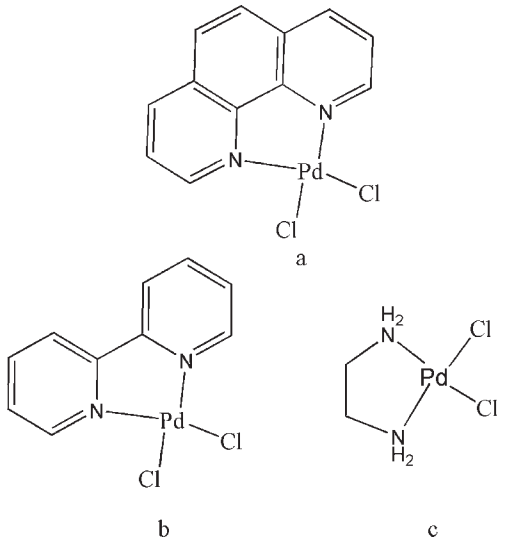

identified to primarily contribute to the high affinity metal binding. Histidyl residues are known to commonly exist in neurodegenerative disease-related proteins including β-amyloid protein (Aβ) and PrP^{Sc}. Their ability to bind metal cations plays a crucial role in neurodegeneration.[24,25] Several studies focused on potential therapeutic applications of metal compounds in the treatment of Alzheimer's disease by targeting the metal binding site and alkylating the imidazole side chains of Aβ.[25−27] In addition, our previous investigation on the interactions of Pt- and Au-based metal complexes with PrP106-126 demonstrated that tetracoordinated Pt and Au complexes affected the conformation of PrP106-126 markedly and inhibited its aggregation, which seems to suggest a new approach to better understanding the design and development of metallodrugs against prion diseases.[28]

Palladium is a soft transition metal, and Pd(II) can bind to some PrP fragments with high binding affinity and site selectivity linked to the involvement of both imidazole and amide nitrogen atoms from the peptide.[29] In addition, Pd complexes were usually investigated as platinum anticancer drugs used to interact with double-stranded DNA (dsDNA), finding that some of them exhibited significant antitumor activity against some tumor cell lines.[30−33] The interaction of Pt, Pd, and Au complexes with protein also reportedly helped develop a better understanding of the modulation of metal-binding protein functions by different metal ions.[34] The aim of the present work was to prepare a series of Pd-based complexes and elucidate their interactions with PrP106-126. The complexes shown in Scheme 1 are composed of Pd(II) with three different ligands: 1,10-phenanthroline (phen, a), 2,2′-bipyridine (bipy, b), and ethylenediamine (en, c). The study was intended to observe changes in PrP106-126 properties induced by different Pd complexes and to clarify the relationship between the ligand properties and aggregation of this active peptide, in the hope of developing novel therapeutic agents against prion diseases.

EXPERIMENTAL SECTION

Materials. Human prion protein fragment PrP106-126 was chemically synthesized by SBS Co., Ltd. (Beijing, China), further purified, and identified by high performance liquid chromatography (HPLC) and mass spectrometry (MS) with more than 95% purity. The sample's purity was also confirmed with a ^{1}H NMR spectrum. The peptide in this study had free C and N termini unless otherwise specified. The Pd complexes were prepared as described previously,[35−38] dissolved in DMSO or d6-DMSO, and stored at −20 °C for later use. All other reagents were of analytical grade.

NMR Spectroscopy. The sample for NMR study was prepared in H_2O containing 10% d6-DMSO. The reaction of PrP106-126 and a Pd complex was performed by adding small aliquots of a metal compound stock solution to the peptide solution. The pH value was carefully adjusted to 5.8 with either HCl or NaOH. The final peptide concentration was 0.4 mM. NMR experiments were carried out on a Bruker Avance 400 MHz spectrometer at 25 °C. Suppression of the residual water signal was achieved by the watergate pulse program with gradients.

Proton spin−lattice relaxation rates were measured in a selective manner (R^{se}) using the $(180°-\tau-90°-t)_n$ sequence in D_2O containing 10% d6-DMSO at pH 5.8 and 25 °C. The pH value was carefully adjusted to 5.8 with either DCl or NaOD. The τ values used for the experiments were 1×10^{-5}, 0.1, 0.2, 0.3, 0.4, 0.5, 0.6, 0.7, 0.8, 1, 1.2, 1.5, 2, 3, and 5.0 s respectively. The delay time t in this case is 5.0 s. The 180° selective inversion of proton spin population was obtained by a selective Gaus1_180i.1000 shape pulse with a length of 20 ms and a power of 50 dB corresponding to an excitation width of about 45 Hz. All NMR data were processed by the Bruker Topspin 2.1 software.

Circular Dichroism Spectroscopy. Circular dichroism (CD) spectra were measured on a Jasco J-810 spectropolarimeter (Japan Spectroscopy Co., Japan). The sample was prepared in a 5 mM phosphate buffer at a pH of 7.2. The final peptide concentration was 0.1 mM, and the molar ratio of the Pd complex to PrP106-126 was 0.2, 0.5, and 1.0, respectively. A 1 mm quartz cell was used for all CD spectra. The spectra were recorded between 190 and 250 nm with a 0.5 nm spectral step and 2 nm of bandwidth. A scan rate of 100 nm min^{-1} with a 1 s response time was employed. The background spectrum was subtracted using the same buffer. The final spectrum for each sample was the average of three repeated experiments.

Electrospray Ionization Mass Spectrometry (ESI-MS). The peptide concentration used in MS determination was constant at 50 μM. An equivalent amount of the Pd complex was incubated with the peptide. ESI-MS spectra were recorded in the positive mode by direct introduction of the samples at a 3 μL min^{-1} flow rate in an APEX IV FT-ICR high-resolution mass spectrometer (Bruker, USA), equipped with a conventional ESI source. The working conditions included the following: end plate electrode voltage, −3500 V; capillary entrance voltage, −4000 V; skimmer 1 voltage, 30 V; and dry gas temperature, 200 °C. The flow rate of the drying gas and the nebulizer gas was set at 12 and 6 L min^{-1}, respectively. The DataAnalysis 4.0 software (Bruker) was used for acquisition, and the deconvoluted masses were obtained using the integrated deconvolution tool.

Thioflavin T(ThT) Assay. An equivalent amount of the Pd complex was added to 0.1 mM PrP106-126 in a 10 mM phosphate buffer, at a pH of 7.2. The sample was incubated with 10 μM ThT, and the sample fluorescence was monitored using an LS55 spectrofluorometer (Perkin-Elmer, USA). The ThT signal was quantitated by averaging the fluorescence emission at 500 nm over 10 s when excited at 432 nm. The reported data were the average of three timed experiments.

Transmission Electron Microscopy (TEM). Samples were prepared by mixing an equivalent of the Pd complex with 5 mM peptide solution and then incubated at 37 °C for 24 h. The final peptide concentration used in the TEM experiment was 0.1 mM with 1% DMSO. An aliquot of each sample was spotted onto a carbon-coated 600-mesh copper grid and negatively stained with 2% phosphotungstic acid. Air-dried specimens were examined and photographed in a Hitachi H-800 electron microscope (Hitachi, Japan) operating at 200 kV.

dx.doi.org/10.1021/ic102331x |Inorg. Chem. 2011, 50, 4340–4348

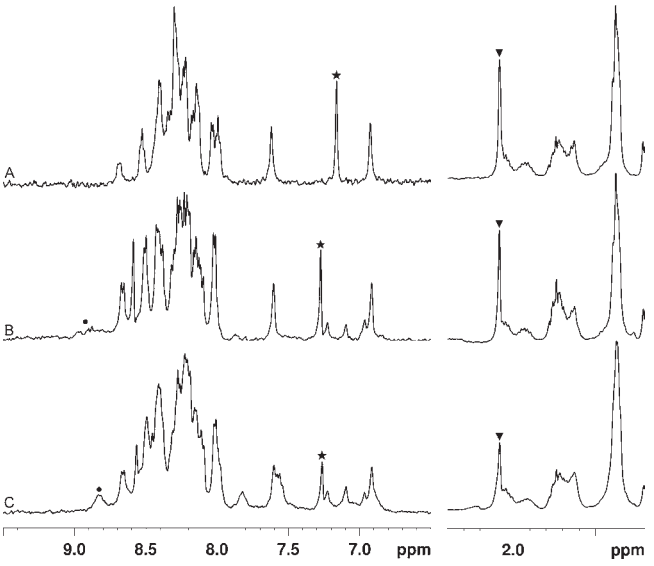

Figure 1. ^{1}H NMR spectra of 0.4 mM PrP106-126 in H_2O/DMSO at a pH of 5.8 and 298 K. PrP106-126 alone (A). PrP106-126 in the presence of 1.0 equiv of Pd(phen)Cl_2 (B) and 1.0 equiv of Pd(bipy)Cl_2 (C). The peak at 2.08 ppm from an $C_\varepsilon H_s$ group of methionine was significantly decreased when it was incubated with Pd(bipy)Cl_2. The peak at 7.16 ppm marked with an asterisk was from the $C_\delta H_s$ of His111. It was obviously perturbed by the metal complex. The dotted peaks at about 8.80 ppm were mainly from the metal complexes.

MTT analysis. Human SH-SY5Y neuroblastoma cells were cultured in Dulbecco's modified Eagle's medium (DMEM) supplemented with 10% fetal bovine serum (FBS), 2 mM glutamine, 100 U mL^{-1} penicillin, and 100 U mL^{-1} streptomycin; cells were maintained at 37 °C in a humidified incubator under 95% air and 5% CO_2. Cell survival was assessed by measuring the reduction of 3-(4,5-dimethylthiazol-2-yl)-2,5-diphenyl-terazolium bromide(MTT).[39−41] The Pd complex and PrP106-126 were added directly to the cells from the stock solution to reach the desired concentration. After 4 days of treatment, cells were incubated for 4 h with 10 μL MTT at 37 °C; the medium was dissolved in DMSO after removal of the upper clean liquid. The absorbance of the final solution was read in a spectrophotometer at 570 nm. Each experiment was carried out in triplicate. The data were calculated as a percentage of untreated vehicle control values.

RESULTS

Interaction of Pd Complexes with PrP106-126 Detected by NMR. To study the interaction of Pd complexes with PrP106-126, ^{1}H NMR spectra were acquired at a pH of 5.8 and at 25 °C, as chosen previously.[20,28,42] As shown in Figure 1, the ^{1}H NMR spectrum of PrP106-126 was confirmed and consistent with the previous result.[20] The increased amount of the Pd complex caused proton resonance line broadening. Incubation of Pd(phen)Cl_2 with PrP106-126 induced a change in the chemical shift of His111$C_\delta H_s$ from 7.16 to 7.29 ppm, suggesting that the most possible binding site of Pd(phen)Cl_2 was at His111. Several new peaks were observed, including those from the free metal complex and those from the bound state of PrP106-126. Compared with Pd(phen)Cl_2, incubation of Pd(bipy)Cl_2 with PrP106-126 caused a change of the resonance representing the $C_\delta H_s$ of His111, and the peak intensity was decreased significantly. In addition, the most significant change in the Pd(bipy)−PrP106-126 complex was the clearly weakened peak at 2.08 ppm, which was assigned to the $C_\varepsilon H_s$ of methionine. The obtained spectrum indicated that Met109 and/or Met112 might be involved in the binding to PrP106-126 and represent an additional binding site for Pd(bipy)Cl_2. In the presence of Pd(en)Cl_2, the $C_\varepsilon H_s$ resonance of methionine residue showed perturbation similar to that of Pd(bipy)Cl_2, while the intensity of the His111 $C_\delta H_s$ resonance was much lower than that of Pd(bipy)Cl_2 (Figure S1, Supporting Information). The decreased peak intensity of the His111 $C_\delta H_s$ and $C_\varepsilon H_s$ groups of methionine indicated the involvement of residues histidine and methionine in the Pd(en)Cl_2 binding to PrP106-126. During the binding process, the peaks assigned to the metal complexes were also shown. Taking Pd(bipy)Cl_2 as an example, the ligand itself had three set of peaks (Figure S2, Supporting Information). In the D_2O solution of PrP106-126, the two downfield peaks were from the side chain of His111. After the peptide was incubated with the Pd complex, several peaks assigned to the ligand from the free and bound states were clearly observed.

Table 1. The 400 MHz ^{1}H NMR Parameters of PrP106-126 (0.4 mM) in D_2O at a pH of 5.8 and T = 25°C in the Absence and Presence of Equivalent Pd Compounds

	PrP106-126	PrP106-126-Pd(phen)Cl_2	PrP106-126-Pd(bipy)Cl_2	PrP106-126-Pd(en)Cl_2
proton	R^{se} (s^{-1})	R^{se} (s^{-1})	R^{se}(s^{-1})	R^{se}(s^{-1})
C_δHs of His111	0.73	0.75	1.73	1.26
C_εHs of Met109/112	1.05	1.06	1.15	1.11
C_βHs of Ala	1.51	1.51	1.51	1.51

The proton spin−lattice relaxation rate has proved to be a very suitable parameter in the ligand−macromolecule complex studies. In particular, the slower rotational tumbling of the ligand−macromolecule complex mainly affects the selective relaxation rate R^{se}.[43,44] To study the binding site property of PrP106-126−Pd complex, the selective relaxation rate experiments were performed for the protons referring to the $C_\delta H_s$ of His111, the $C_\varepsilon H_s$ of Met109/112, and the overlapped $C_\beta H_s$ of Ala residues. The results are shown in Table 1. For the protons of His111, the selective relaxation rates were increased to different extents after PrP106-126 was incubated with three Pd complexes. While for Met109/112 $C_\varepsilon H_s$, the rates were increased obviously after adding Pd(bipy)Cl_2 or Pd(en)Cl_2. However, the rate of Ala $C_\beta H_s$ was unchanged in the absence and presence of the Pd complex. The NMR data indicate that Pd complexes interacted with PrP106-126, and the differences between these spectral parameters implied that the binding mode of Pd complexes might be different.

PrP106-126 Conformational Changes Induced by Pd Complexes. CD spectroscopy was employed to examine the effect of Pd complexes on the conformation of PrP106-126 at physiological pH. The peptide in a 5 mM phosphate buffer at a pH of 7.2 gave a predominately negative CD absorbance at 197 nm as the typical random coil structure. It also showed negative ellipticities in the region of 210−230 nm, slightly different from that of random coil (Figure 2A), suggesting that the peptide was characterized by the presence of small amounts of secondary structure elements. The addition of equivalent Pd complexes

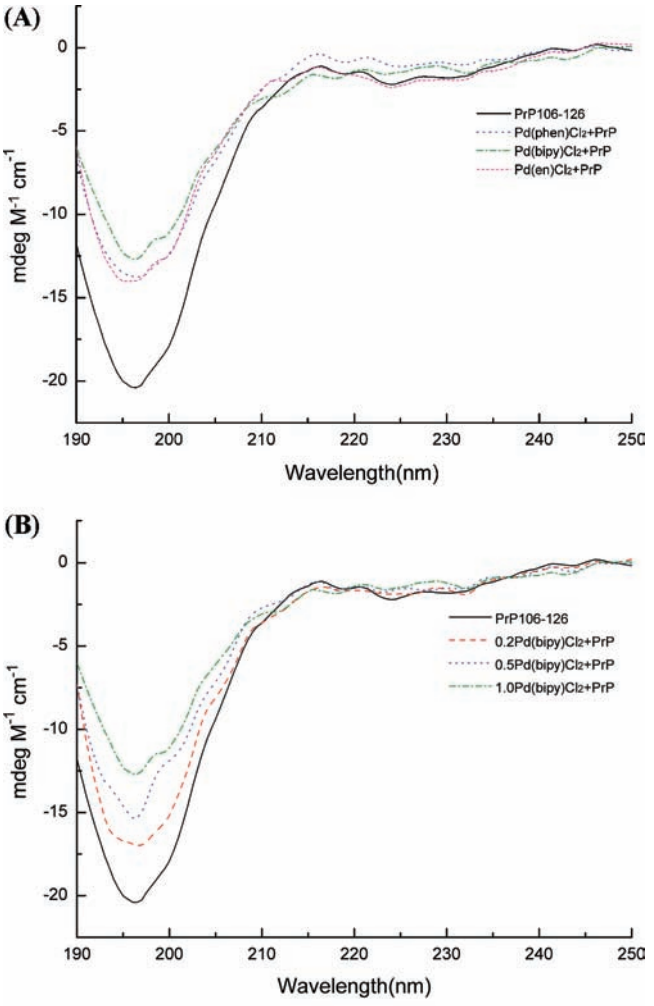

Figure 2. Circular dichroism spectra of the PrP106-126 (solid line) and in the presence of different 1.0 equiv of Pd complexes (A) and different concentrations of $Pd(bipy)Cl_2$ (B). The PrP106-126 concentration in solution was 0.1 mM.

induced a decrease of the negative CD absorbance at 197 nm. Comparisons of the CD spectra showed a shoulder peak emerging around 200 nm after the addition of Pd complexes, except for $Pd(phen)Cl_2$. $Pd(bipy)Cl_2$ displayed the most effective change in the PrP106-126 conformation. Figure 2B shows a gradient change of the PrP106-126 CD spectra with a molar ratio of $Pd(bipy)Cl_2$ to PrP106-126 at 0, 0.2, 0.5, and 1.0. It is interesting that the shoulder peak did not appear until 0.5 equiv of $Pd(bipy)Cl_2$ was added, and the peak was strengthened via adding more $Pd(bipy)Cl_2$. Although it was not easy to clearly define the conformational change of PrP106-126, these data indicate that the Pd complexes could dramatically influence the solution conformation of the peptide.[40]

ESI-MS Study on the Binding of Pd Complexes to PrP106-126. To determine whether the Pd complexes bound directly to PrP106-126, equivalent amounts of Pd complexes (**1a**−**1c**) were incubated with the peptide, and the final solution was analyzed by ESI-MS. The resulting ESI-MS deconvoluted spectra are shown in Figure 3. The free PrP106-126 exhibited an intense peak at 1911 ± 1 Da, corresponding to its expected mass (Figure 3A). Surprisingly, the spectra exhibited different appearances after different Pd complexes were incubated with PrP106-126. Figure 3B shows that treatment of the peptide with $Pd(phen)Cl_2$ led to the appearance of additional peaks at 2198 ± 1 Da and 2230 ± 1 Da, which were straightforwardly assigned to the metal−peptide adducts. The increase in mass of 287 and 319 Da matched the fragments $Pd(phen)^{2+}$ and $Pd(phen)Cl^{+}$, respectively, suggesting that the compound bound to the PrP106-126 at a ratio of 1:1 and the two chloro ligands were displaced one by one in solution. Incubation of $Pd(bipy)Cl_2$ with the PrP fragment (Figure 3C) produced a different spectrum with new intense peaks centered at 2169 ± 1 Da and 2430 ± 1 Da, indicating that the $Pd(bipy)^{2+}$ bound to PrP106-126 at a ratio of 1:1 and 2:1, respectively. The two chloro ligands in $Pd(bipy)Cl_2$ were displaced during the formation of the two adducts. The mass spectrum from the incubation of $Pd(en)Cl_2$ with PrP106-126 (Figure 3D) showed that the formation of the adducts was similar to that of $Pd(bipy)Cl_2$. The detected mass peaks matched the PrP106-126-Pd complex very well, indicating a higher binding affinity of these Pd complexes. No fragmented peptide was found to identify the exact residue to which the Pd complex was coordinated. Moreover, the mass increase of 32 or 16 corresponding to the oxidation of the Met side chain to sulfoxides was not observed either, suggesting that the S center of the Met residue is in a possible coordination state.[45] The MS data indicate that these Pd complexes bound to PrP106-126 in a different binding mode, which is consistent with that found in the NMR study.

ThT Analysis of PrP106-126 Aggregation Induced by Pd Complexes. PrP106-126 is essential to the aggregation of PrP^{Sc}, which is correlated with the prion protein toxicity. The aggregation of PrP106-126 can be monitored by ThT assay, which gave rise to a new excitation at 432 nm and enhanced emission at 500 nm.[40] As shown in Figure 4, the spectrum gave a strong fluorescence signal when ThT bound to PrP106-126. However, after incubation with Pd complexes, ThT fluorescence was decreased significantly, suggesting that the formation of the fibril structure was inhibited effectively after the addition of the Pd complexes. Three Pd complexes have no absorption at 500 nm in UV spectra (data not shown). This indicates that the change of fluorescence intensity is induced by the binding of Pd complexes to PrP106-126. Further, it is not difficult to discover that in the presence of $Pd(bipy)Cl_2$ and $Pd(phen)Cl_2$, PrP106-126 had weaker fluorescence than that of $Pd(en)Cl_2$, indicating that the aggregation of PrP106-126 was better inhibited by $Pd(bipy)Cl_2$ and $Pd(phen)Cl_2$.

PrP106-126 Aggregation Image by TEM. The TEM method was also performed to ascertain whether the Pd complexes affected peptide aggregation and fibril formation (Figure 5). After 24 h of incubation at 37 °C, the aggregate formed by PrP106-126 was the same as that reported previously.[28] However, the electron micrographs of PrP106-126 in the presence of the Pd complexes showed that the aggregation was reversed to a different extent. It was notable that $Pd(bipy)Cl_2$ significantly reversed the aggregation of PrP106-126, and the morphology appeared as thin long hair. In the presence of $Pd(phen)Cl_2$, the negatively stained fibrils were more branched and more intensive than that of $Pd(bipy)Cl_2$. When PrP106-126 was incubated with $Pd(en)Cl_2$, it represented a conservative modification with similar aggregation to the PrP−$Pd(phen)Cl_2$ system.

Pd Complexes Regulate the Neurotoxicity of PrP106-126. Knowing that the Pd complexes could bind to PrP106-126, change the solution conformation of the active peptide, and modify fibril generation, their ability to inhibit neurotoxicity of

dx.doi.org/10.1021/ic102331x |*Inorg. Chem.* 2011, 50, 4340–4348

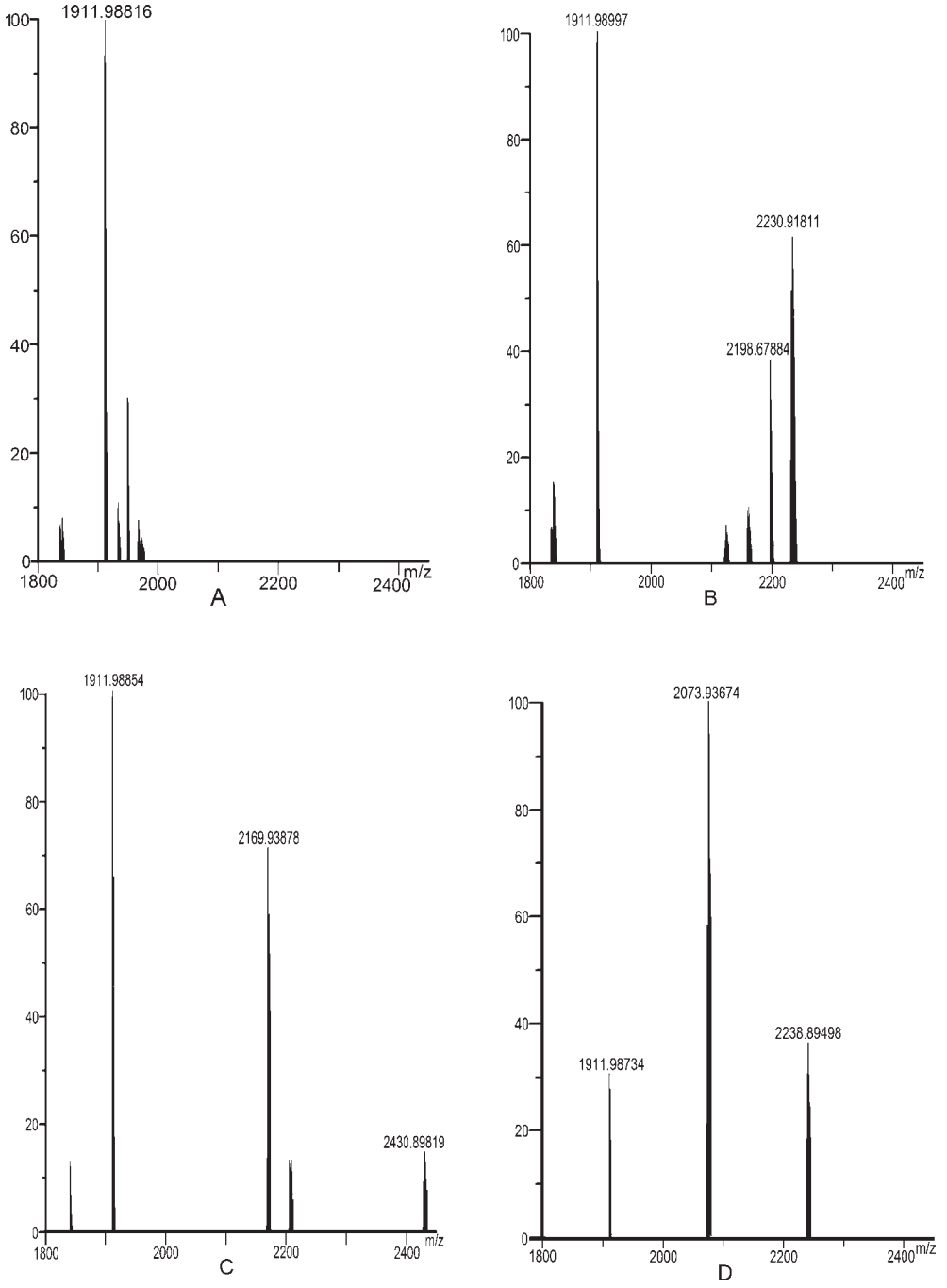

Figure 3. Deconvoluted ESI-MS spectra of PrP106-126 in the absence (A) and presence of $Pd(phen)Cl_2$ (B), $Pd(bipy)Cl_2$ (C), and $Pd(en)Cl_2$ (D). The aqueous mixture was prepared by adding equivalent amounts of Pd complexes to PrP106-126. The solution was diluted in water to a final concentration of 50 μM.

the peptide to human SH-SY5Y neuroblastoma cells was finally assessed. Cell survival was evaluated after prolonged treatment with PrP106-126 alone or with the PrP−Pd complex system for 4 days. Pd complexes were not toxic at the tested concentration (1 μM).

Compared with the control sample, PrP106-126 (100 μM) caused a significant reduction of cell viability to 71% of the control as measured by MTT assay (Figure 6). Coincubation of 1 μM Pd complexes with PrP106-126 restored and upregulated the cell viability. $Pd(bipy)Cl_2$ significantly reduced cell toxicity of the peptide, resulting in an increase of cell viability to 89% of the control. The other two compounds also decreased the toxicity of PrP106-126, with cell viability restoring to 75% of the control for $Pd(en)Cl_2$ and to 78% of the control for $Pd(phen)Cl_2$, although they were less active than $Pd(bipy)Cl_2$.

DISCUSSION

Significant efforts have been made to investigate the possible effects of divalent metal ions on biological and physiochemical

dx.doi.org/10.1021/ic102331x |*Inorg. Chem.* 2011, 50, 4340–4348

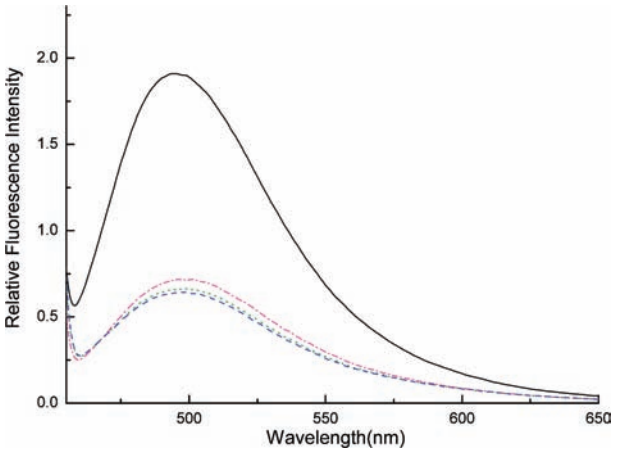

Figure 4. Evaluation of the ability of the Pd complexes to inhibit PrP106-126 aggregation as measured by ThT fluorescence. PrP106-126 was incubated with ThT in the absence (black) and presence of $Pd(phen)Cl_2$ (blue), $Pd(bipy)Cl_2$ (green), and $Pd(en)Cl_2$ (pink).

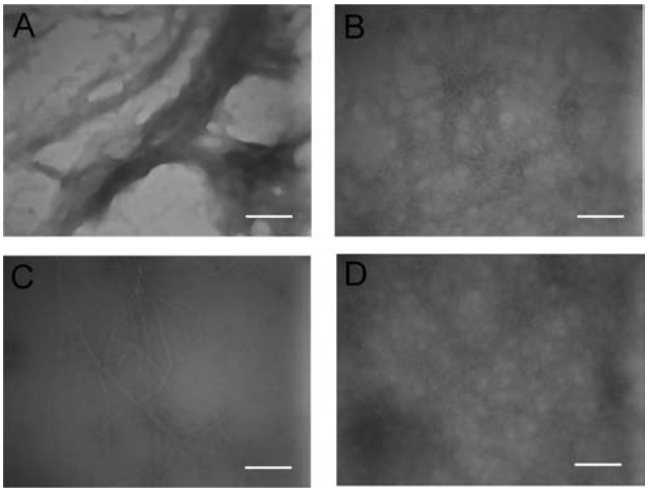

Figure 5. TEM images of PrP106-126 fibrils in the absence (A) and presence of $Pd(phen)Cl_2$ (B), $Pd(bipy)Cl_2$ (C), and $Pd(en)Cl_2$ (D). The scale bar is 200 nm.

properties of PrP fragments.[46−48] PrP106-126 maintains the amyloidogenic and neurotoxic properties of the entire pathological PrP^{Sc} and is usually used as a reasonable model to study the mechanism of prion diseases. The histidine residue is defined as the major binding site in the interaction of PrP106-126 with Cu(II), Mn(II), and Ni(II).[20,23,42] Divalent cations interact with PrP106-126, but their influence on peptide aggregation is limited. Our previous study demonstrated that Pt- and Au-based complexes altered the solution properties of PrP106-126 and inhibited prion fragment aggregation significantly.[28] However, the influence of the ligand property on peptide aggregation is not clearly understood. In this work, Pd complexes inhibited the aggregation of PrP106-126, and the ligand spatial effect was identified to be more important than the binding affinity.

Different Binding Mode of Pd Complexes to PrP106-126. The transition metal ion Pd(II) was reported to be able to bind with several histidine-containing prion peptide fragments.[29] In this work, we used Pd complexes to target the imidazole side

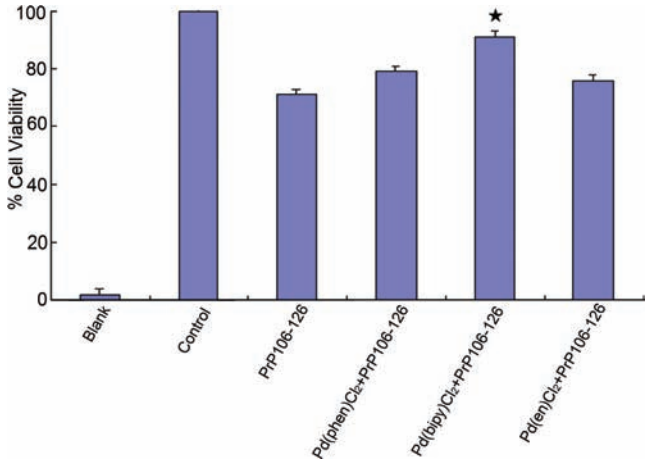

Figure 6. Inhibition of PrP106-126-induced neurotoxicity. Human SH-SY5Y cells were treated with 100 μM PrP 106-126 for 4 days. The addition of 1 μM Pd complexes inhibited the toxicity of PrP106-126. Cell viability was determined with a MTT test. Data represent the average of three experiments. The star represents the most effective cell viability when treated with $Pd(bipy)Cl_2$.

chain and change the physicochemical properties of PrP106-126 and found that these complexes were able to bind to the peptide and modify aggregation of the peptide. NMR and ESI-MS spectra indicate that Pd complexes could bind to PrP106-126 in different binding modes. $Pd(phen)Cl_2$ bound with PrP106-126 at a ratio of 1:1, and the two chloro ligands were displaced.

From the analysis of relaxation rates, $Pd(phen)Cl_2$ might coordinate with the N_{im} atom of His111 and another amide nitrogen atom, but not with methionine, since the relaxation property of methionine $C_\varepsilon H_s$ was not changed in the $Pd(phen)Cl_2$−PrP106-126 system. In addition, the hydrophobic region (A113−G126) may not participate in the binding process, as the selective relaxation rate of Ala $C_\beta H_s$ was unchanged in the absence and presence of the Pd complex.

Differently, both $Pd(bipy)Cl_2$ and $Pd(en)Cl_2$ bound to PrP106-126 at a ratio of 2:1. To confirm the binding mode of the Pd complex to PrP106-126, 1D NMR titration experiments were carried out for the $Pd(bipy)Cl_2$−PrP106-126 system. The titration results from the peak referring to the $C_\varepsilon H_s$ of methionine (109/112) showed a 2:1 binding stoichiometry for the system (Figure S3, Supporting Information). Incubation of PrP106-126 with $Pd(bipy)Cl_2$ or $Pd(en)Cl_2$ reduced the intensity of His111 $C_\delta H_s$ and methionine (119 and/or 112) $C_\varepsilon H_s$. This was also verified by the proton relaxation results. Furthermore, the 2D TOCSY spectra of the PrP106-126−Pd complex did not display obvious differences from the chemical shift change of Met109 and Met112 (data not shown). Therefore, it is reasonable to deduce that His111, Met112, and Met109 contribute to the coordination of $Pd(bipy)Cl_2$ and $Pd(en)Cl_2$. Another coordination site might also be from the amide nitrogen atom.

Different binding modes were also reflected by CD spectra. The coordination of Pd complexes to PrP106-126 significantly changed the secondary structure of the peptide. An interesting observation from our conformational study is that a shoulder peak emerged around 200 nm after the addition of $Pd(bipy)Cl_2$ and $Pd(en)Cl_2$, rather than in the Pd(phen)−PrP system, even at a higher concentration of $Pd(phen)Cl_2$ (Figure S4, Supporting Information). With the results obtained from the MS and NMR experiments considered, it is not difficult to understand why the

dx.doi.org/10.1021/ic102331x |*Inorg. Chem.* 2011, 50, 4340–4348

interaction of PrP106-126 with Pd(bipy)Cl_2 or Pd(en)Cl_2 resulted in a peptide conformation slightly different from that resulting from treatment with Pd(phen)Cl_2.

Effective Inhibition of Pd Complexes on PrP106-126 Aggregation and Neurotoxity. To better correlate the physical state with neurotoxicity of the peptide, its aggregation properties were investigated in the presence of the Pd complexes by ThT assay and TEM. The results showed that all complexes reversed the fibril formation. Interestingly, the three compounds had a relatively similar inhibitory effect on PrP106-126 when detected in a solution state (ThT). But the inhibitory effect was different when it was determined by TEM. This may be induced by different spatial orientations when different metal complexes (particularly different ligands) bind to the peptide in a different mode, and the orientation is more effective on peptide aggregation on the film (TEM). In a word, Pd(bipy)Cl_2 is most effective in inhibiting the aggregation of PrP106-126.

As mentioned above, the difference of solution pH (5.8 and 7.2) between NMR and CD/ThT experiments does not affect the binding property and the aggregation behavior of Pd complex to PrP106-126, obviously. In addition, the most essential test for the potential efficacy of the Pd complexes is their ability to inhibit the PrP106-126 neurotoxicity in a cellular system. We therefore assessed their ability to reduce PrP106-126-induced toxicity in human SH-SY5Y neuroblastoma cells. Despite the high toxicity of Pd(II) compounds as was believed, Pd complexes increased cell viability and decreased PrP106-126-induced cell toxicity in the present cellular system. Pd(bipy)Cl_2 has the most potential of the complexes studied in reversing aggregation and reducing neurotoxicity.

Comparison of a Single Pd(II) Cation with Three Pd Complexes on Binding to PrP106-126. The interactions of the three Pd complexes with PrP106-126 were well indicated in this work. However, the problem of why different ligands affect aggregation to different extents remains. Did a single Pd(II) cation inhibit the aggregation of PrP106-126 effectively? We then studied the interaction between K_2PdCl_4 and PrP106-126 under the same conditions. In the ESI-MS spectrum, the peak assigned to the peptide disappeared, and new peaks were observed at 2013 ± 1 Da and 2118 ± 1 Da, which corresponded to the formation of Pd−PrP106-126 and Pd_2−PrP106-126 adducts, respectively (Figure S5, Supporting Information).

The NMR and CD spectra of the Pd−PrP106-126 complex were similar to that of Pd(en)−PrP106-126 (Figures S1 and S6, Supporting Information). Moreover, the results of ThT assay showed that K_2PdCl_4 decreased ThT fluorescence markedly, although this decrease was less than that of Pd(bipy)Cl_2 (Figure S7, Supporting Information). The TEM experiment also showed a result similar to that for Pd(en)Cl_2 (Figure S8, Supporting Information), indicating that K_2PdCl_4 had a similar inhibitory effect on PrP106-126 aggregation to that of Pd(en)Cl_2.

In fact, Pd(II) was reported to bind to other PrP fragments with a high binding affinity,[29] which was also confirmed by our MS spectrum when it bound to PrP106-126. Compared with K_2PdCl_4, the mass peak intensity at 1912 for the peptide declined gradually after the peptide was incubated with Pd(phen)Cl_2, Pd(bipy)Cl_2, and Pd(en)Cl_2. On the other hand, the peak intensity for the Pd−peptide complexes increased step by step. These data present a binding affinity in the order of K_2PdCl_4 > Pd(en)Cl_2 > Pd(bipy)Cl_2 > Pd(phen)Cl_2, which is in accordance with the theoretical speculation for Pd complexes: (1) The planar aromatic heterocyclic rings 1,10-phenan-throline and 2,2′-bipyridine are conjugated electron-rich systems and may weaken the coordination ability of Pd(II) to PrP106-126. (2) As the ligand ethylenediamine does not have an extra conjugated π electron, the coordination ability of Pd(II) would not be affected significantly.

To identify the binding affinity of Pd(II)/Pd complexes to PrP106-126, the NMR experiments were performed using Cu(II) and Mn(II) as controls.[42] According to the reported works, the binding constants of Cu(II) and Mn(II) to PrP106-126 are about 10^{15} and 10^4, respectively.[23,42] The paramagnetic Cu(II) will cause the peak of His111 $C_\delta H_s$ to disappear after binding to the N_{im} of His111, whereas Pd(II) is diamagnetic. The featured peak of His111 $C_\delta H_s$ changed differently when K_2PdCl_4 or Pd(en)Cl_2 was added to the peptide solution (Figure S1, Supporting Information). Cu(II) could not interfere in the binding of Pd(II) or Pd(en)Cl_2 to PrP106-126. Interestingly, the featured peak disappeared in the Pd(phen)Cl_2−PrP106-126−Cu system, just like when Cu(II) was added alone (Figure S9, Supporting Information). These NMR competition experiments present a binding affinity in the order of K_2PdCl_4 > Pd(en)Cl_2 ≫Cu(II) > Pd(bipy)Cl_2 ≫ Mn(II) > Pd(phen)Cl_2. The results reveal that different physiochemical properties of the Pd complexes with respect to PrP106-126 binding might be caused by the variety of ligands.

Role of the coordinated ligand in PrP106-126 aggregation. Studies showed that although K_2PdCl_4 and Pd(en)Cl_2 had a high binding affinity to PrP106-126, their inhibition on PrP106-126 aggregation was not satisfactory. The hydrophobic C-terminal residues from 113 to 126 were stacked during PrP aggregation, and Met112 was a crucial site that might reverse the aggregation process.[19,28,40] Our NMR data indicated that methionine was an additional binding site besides the imidazole nitrogen atom of His111 for Pd complexes except Pd(phen)Cl_2, and the two Met residues might both participate in coordination of the three compounds in binding to PrP106-126 at a ratio of 2:1. The inhibitory effect of Pd(bipy)Cl_2 on PrP106-126 aggregation may be attributable to the steric effect of the bipy ligand by occupying a larger space and inhibiting the stack of interface of hydrophobic C-terminal residues. As for K_2PdCl_4, however, its strong binding to PrP106-126 could not prevent the aggregation effectively, implying that the binding site is near the hydrophilic region of the peptide and the Pd/Pd_2−PrP106-126 complex has not enough steric effect on inhibiting the hydrophobic C-terminal stack. In addition, as the phen ligand is large enough, the relatively weaker binding affinity of Pd(phen)Cl_2 to PrP106-126 influences peptide aggregation more than what we image. Therefore, it may not be the high binding affinity but the large space obstacle of Pd complexes that produces the ideal inhibitory effect on PrP aggregation.

SUMMARY

The interactions of Pd complexes with PrP106-126 indicate that three Pd complexes could bind to PrP106-126 in different binding modes and inhibit peptide aggregation significantly. It provides new experimental data to understand the influence of metal complexes on neuropeptide biological and physiochemical property. The differences from these Pd complexes on peptide aggregation demonstrate that adequate ligand coordination is essential. More consideration should be given to the ligand spatial effects on peptide conformation and the behavior of PrP aggregation rather on high binding affinity. Further works are under investigation to synthesize the most potent metal complex and

get a detailed structural analysis of the peptide/metal complex. In addition, the mechanism of PrP106-126 and PrP^{Sc} toxicity is complicated, which might involve multiple factors, including peptide aggregation and metal ion coordination. Our results may be valuable in helping design and develop novel metallodrugs against prion diseases.

■ ASSOCIATED CONTENT

Supporting Information. NMR, MS, CD, FL, and TEM data for the Pd(II)−PrP106-126 system; NMR data for the $Pd(en)Cl_2$−PrP106-126 system; CD spectra of $Pd(phen)Cl_2$−PrP106-126 in different molar ratios; and a comparison of $Pd(phen)Cl_2$ with Cu(II) and Mn(II) on binding affinity to PrP106-126. This material is available free of charge via the Internet at http://pubs.acs.org.

■ AUTHOR INFORMATION

Corresponding Author

*Tel./Fax: 8610-6251-2660/6444. E-mail: whdu@chem.ruc.edu.cn; ymlius@163.com.

Author Contributions

§These authors contributed equally to this paper.

■ ACKNOWLEDGMENT

This work was supported by the National Basic Research Program (No. 2011CB808503), Shanghai Eastern Scholar Grant for Y.Li from Shanghai Education Commission (2008), and the Fundamental Research Funds for the Central Universities and the Research Funds of Renmin University of China (No. 10XNJ011).

■ REFERENCES

(1) Prusiner, S. B. *Science* **1997**, *278*, 245–251.
(2) Prusiner, S. B. *Proc. Natl. Acad. Sci. U.S.A.* **1998**, *95*, 13363–13383.
(3) Diedrich, J. F.; Bendheim, P. E.; Kim, Y. S.; Carp, R. I.; Haase, A. T. *Proc. Natl. Acad. Sci. U.S.A.* **1991**, *88*, 375–379.
(4) Stahl, N.; Borchelt, D. R.; Hsiao, K.; Prusiner, S. B. *Cell* **1987**, *51*, 229–240.
(5) Korth, C.; Stierli, B.; Streit, P.; Moser, M.; Schaller, O.; Fischer, R.; Schulz-Schaeffer, W.; Kretzschmar, H.; Raeber, A.; Braun, U.; Ehrensperger, F.; Hornemann, S.; Glockshuber, R.; Riek, R.; Billeter, M.; Wüthrich, K.; Oesch, B. *Nature* **1997**, *390*, 74–77.
(6) Pan, K. M.; Baldwin, M.; Nguyen, J.; Gasset, M.; Serban, A.; Groth, D.; Mehlhorn, I.; Huang, Z.; Fletterick, R. J.; Cohen, F. E.; Prusiner, S. B. *Proc. Natl. Acad. Sci. U.S.A.* **1993**, *90*, 10962–10966.
(7) Stanczak, P.; Kozlowski, H. *Biochem. Biophys. Res. Commun.* **2007**, *352*, 198–202.
(8) Aguzzi, A.; Baumann, F.; Bremer, J. *Annu. Rev. Neurosci.* **2008**, *31*, 439–477.
(9) Jobling, M. F.; Stewart, L. R.; White, A. R.; McLean, C.; Friedhuber, A.; Maher, F.; Beyereuther, K.; Masters, C. L.; Barrow, C. J.; Collins, S. J.; Cappai, R. *J. Neurochem.* **1999**, *73*, 1557–1565.
(10) Tagliavini, F.; Prelli, F.; Verga, L.; Giaccone, G.; Sarma, R.; Gorevic, P.; Ghetti, B.; Passerini, F.; Ghibaudi, E.; Forloni, G.; Salmona, M.; Bugiani, O.; Frangione, B. *Proc. Natl. Acad. Sci. U.S.A.* **1993**, *90*, 9678–9682.
(11) Brown, D. R.; Schmidt, B.; Kretzschmar, H. A. *Nature* **1996**, *380*, 345–347.
(12) Vella, L.; Hill, A. F.; Cappai, R. *Neurodegener. Prion Dis.* **2005**, 217–240.
(13) Chabry, J.; Ratsimanohatra, C.; Sponne, I.; Elena, P. P.; Vincent, J. P.; Pillot, T. *J. Neurosci.* **2003**, *23*, 462–469.
(14) Brown, D. R. *Biochem. J.* **2000**, *352*, 511–518.
(15) Rymer, D. L.; Good, T. A. *J. Neurochem.* **2000**, *75*, 2536–2545.
(16) Selvaggini, C.; De Gioia, L.; Cantù, L.; Ghibaudi, E.; Diomede, L.; Passerini, F.; Forloni, G.; Bugiani, O.; Tagliavini, F.; Salmona, M. *Biochem. Biophys. Res. Commun.* **1993**, *194*, 1380–1386.
(17) Chiti, F.; Dobson, C. M. *Annu. Rev. Biochem.* **2006**, *75*, 333–366.
(18) Grabenauer, M.; Wu, C.; Soto, P.; Shea, J. E.; Bowers, M. T. *J. Am. Chem. Soc.* **2010**, *132*, 532–539.
(19) Walsh, P.; Neudecker, P.; Sharpe, S. *J. Am. Chem. Soc.* **2010**, *132*, 7684–7695.
(20) Gaggelli, E.; Bernardi, F.; Molteni, E.; Pogni, R.; Valensin, D.; Valensin, G.; Remelli, M.; Luczkowski, M.; Kozlowski, H. *J. Am. Chem. Soc.* **2005**, *127*, 996–1006.
(21) Jobling, M. F.; Huang, X. D.; Stewart, L. R.; Barnham, K. J.; Curtain, C.; Volitakis, I.; Perugini, M.; White, A. R.; Cherny, R. A.; Masters, C. L.; Barrow, C. J.; Collins, S. J.; Bush, A. I.; Cappai, R. *Biochemistry* **2001**, *40*, 8073–8084.
(22) Kozlowski, H.; Janicka-Klos, A.; Brasun, J.; Gaggelli, E.; Valensin, D.; Valensin, G. *Coordin. Chem. Rev.* **2009**, *253*, 2665–2685.
(23) Turi, I.; Kallay, C.; Szikszai, D.; Pappalardo, G.; Natale, G. D.; De Bona, P.; Rizzarelli, E.; Sovago, I. *J. Inorg. Biochem.* **2010**, *104*, 885–891.
(24) Cuajungco, M. P.; Frederickson, C. J.; Bush, A. I. *Subcell Biochem.* **2005**, *38*, 235–254.
(25) Barnham, K. J.; Kenche, V. B.; Ciccotosto, G. D.; Smith, D. P.; Tew, D. J.; Liu, X.; Perez, K.; Cranston, G. A.; Johanssen, T. J.; Volitakis, I.; Bush, A. I.; Masters, C. L.; White, A. R.; Smith, J. P.; Cherny, R. A.; Cappai, R. *Proc. Natl. Acad. Sci. U.S.A.* **2008**, *105*, 6813–6818.
(26) Storr, T.; Merkel, M.; Song-Zhao, G. X.; Scott, L. E.; Green, D. E.; Bowen, M. L.; Thompson, K. H.; Patrick, B. O.; Schugar, H. J.; Orvig, C. *J. Am. Chem. Soc.* **2007**, *129*, 7453–7463.
(27) Valensin, D.; Anzini, P.; Gaggelli, E.; Gaggelli, N.; Tamasi, G.; Cini, R.; Gabbiani, C.; Michelucci, E.; Messori, L.; Kozlowski, H.; Valensin, G. *Inorg. Chem.* **2010**, *49*, 4720–4722.
(28) Wang, Y.; Xu, J.; Wang, L.; Zhang, B.; Du, W. *Chem.—Eur. J.* **2010**, *16*, 13339–13342.
(29) Jószai, V.; Nagy, Z.; Ösz, K.; Sanna, D.; Di Natale, G.; La Mendola, D.; Pappalardo, G.; Rizzarelli, E.; Sóvágó, I. *J. Inorg. Biochem.* **2006**, *100*, 1399–1409.
(30) Sönmez, M.; Çelebi, M.; Yardim, Y.; Şentürk, Z. *Eur. J. Med. Chem.* **2010**, *45*, 4215–4220.
(31) Mansuri-Torshizi, H.; Srivastava, T. S.; Chavan, S. J.; Chitnis, M. P. *J. Inorg. Biochem.* **1992**, *48*, 63–70.
(32) Padhye, S.; Afrasiabi, Z.; Sinn, E.; Fok, J.; Mehta, K.; Rath, N. *Inorg. Chem.* **2005**, *44*, 1154–1156.
(33) Gao, E.; Zhu, M.; Liu, L.; Huang, Y.; Wang, L.; Shi, C.; Zhang, W.; Sun, Y. *Inorg. Chem.* **2010**, *49*, 3261–3270.
(34) de Paula, Q. A.; Mangrum, J. B.; Farrell, N. P. *J. Inorg. Biochem.* **2009**, *103*, 1347–1354.
(35) Fanizzi, F. P.; Natile, G.; Lanfranchi, M.; Tiripicchio, A.; Laschi, F.; Zanello, P. *Inorg. Chem.* **1996**, *35*, 3173–3182.
(36) McCormick, B. J.; Jaynes, E. N., Jr.; Kaplan, R. I. *Inorg. Synth.* **1972**, *13*, 216–218.
(37) Wimmer, S.; Castan, P.; Wimmer, F. L.; Johnson, N. P. *J. Chem. Soc., Dalton Trans.* **1989**, *3*, 403–412.
(38) Tercero-Moreno, J. M.; Matilla-Hernández, A.; González-García, S.; Niclós-Gutiérrez, J. *Inorg. Chim. Acta* **1996**, *253*, 23–29.
(39) O'Donovan, C. N.; Tobin, D.; cotter, T. G. *J. Biol. Chem.* **2001**, *276*, 43516–43523.
(40) Florio, T.; Paludi, D.; Villa, V.; Principe, D. R.; Corsaro, A.; Millo, E.; Damonte, G.; D'Arrigo, C.; Russo, C.; Schettini, G.; Aceto, A. *J. Neurochem.* **2003**, *85*, 62–72.
(41) Thellung, S.; Villa, V.; Corsaro, A.; Arena, S.; Millo, E.; Damonte, G.; Benatti, U.; Tagliavini, F.; Florio, T.; Schettini, G. *Neurobiol. Dis.* **2002**, *9*, 69–81.

(42) Belosi, B.; Gaggelli, E.; Guerrini, R.; Kozłowski, H.; Luczkowski, M.; Mancini, F. M.; Remelli, M.; Valensin, D.; Valensin., G. *ChemBioChem* **2004**, *5*, 349–359.
(43) Veglia, G.; Delfini, M.; Del Giudice, M. R.; Gaggelli, E.; Valensin, G. *J. Magn. Reson.* **1998**, *130*, 281–286.
(44) Li, Y. M.; Yin, G. W.; Wei, W.; Wang, H. B.; Jiang, S. H.; Zhu, D. Y.; Du, W. H. *Biophys. Chem.* **2007**, *129*, 212–217.
(45) Heegaarda, P. M. H.; Pedersena, H. G.; Flinkb, J.; Boasa, U. *FEBS Lett.* **2004**, *577*, 127–133.
(46) Remelli, M.; Donatoni, M.; Guerrini, R.; Janicka, A.; Pretegiani, P.; Kozłowski, H. *Dalton Trans.* **2005**, *17*, 2876–2885.
(47) Kozłowski, H.; Janicka-Kłos, A.; Stanczak, P.; Valensin, D.; Valensin, G.; Kulon, K. *Coord. Chem. Rev.* **2008**, *252*, 1069–1078.
(48) Burns, C. S.; Aronoff-Spencer, E.; Legname, G.; Prusiner, S. B.; Antholine, W. E.; Gerfen, G. J.; Peisach, J.; Millhauser, G. L. *Biochemistry* **2003**, *42*, 6794–6803.